

# Automated Analysis of Vitreous Inflammation Using Spectral-Domain Optical Coherence Tomography

Pearse A. Keane<sup>1</sup>, Konstantinos Balaskas<sup>2</sup>, Dawn A. Sim<sup>1</sup>, Kiran Aman<sup>2</sup>, Alastair K. Denniston<sup>3,4,5</sup>, Tariq Aslam<sup>2,6,7</sup>, and for the EQUATOR Study Group\*

<sup>1</sup> NIHR Biomedical Research Centre for Ophthalmology, Moorfields Eye Hospital NHS Foundation Trust and UCL Institute of Ophthalmology, London, UK

<sup>2</sup> Manchester Royal Eye Hospital, Central Manchester University Hospitals NHS Foundation Trust, Manchester Academic Health Science Centre, Manchester, UK

<sup>3</sup> Queen Elizabeth Hospital Birmingham, University Hospitals Birmingham NHS Foundation Trust, Birmingham, UK

<sup>4</sup> Centre for Translational Inflammation Research, College of Medical and Dental Sciences, University of Birmingham, Edgbaston, Birmingham, UK

<sup>5</sup> Birmingham & Midland Eye Centre, Sandwell and West Birmingham NHS Trust, Birmingham, UK

<sup>6</sup> Faculty of Medical and Human Sciences, University of Manchester, UK

<sup>7</sup> School of Built Environment, Herriot-Watt University, UK

**Correspondence:** Alastair K. Denniston, Queen Elizabeth Hospital Birmingham, University Hospitals Birmingham NHS Foundation Trust, Birmingham, United Kingdom; a.denniston@bham.ac.uk

**Received:** 18 March 2015

**Accepted:** 27 April 2015

**Published:** 16 September 2015

**Keywords:** vitreous inflammation; optical coherence tomography; uveitis automated segmentation

**Citation:** Keane PA, Balaskas K, Sim DA, et al. Automated Analysis of Vitreous Inflammation Using Spectral Domain Optical Coherence Tomography. 2015;4(5):4, doi:10.1167/tvst.4.5.4

**Purpose:** To develop an automated method for quantifying vitreous signal intensity on optical coherence tomography (OCT), with particular application for use in the assessment of vitreous inflammation.

**Methods:** This retrospective, observational case-control series comprised 30 patients (30 eyes), with vitreous haze secondary to intermediate, posterior, or panuveitis; 12 patients (12 eyes) with uveitis without evidence of vitreous haze; and 18 patients (18 eyes) without intraocular inflammation or vitreoretinal disease. The presence and severity of vitreous haze was classified according to the National Eye Institute system; other inflammatory indices and clinical parameters were also documented. Spectral-domain OCT images were analyzed using custom VITreous ANalysis software (termed 'VITAN'), which is fully automated and avoids the need for manual segmentation.

**Results:** VITAN performed accurate segmentation in all scans. Automated measurements of the vitreous:retinal pigment epithelium (RPE) signal ratio showed a moderate correlation with clinical vitreous haze scores ( $r = 0.585$ ,  $P < 0.001$ ), comparable to that reported using manual segmentation in our previous study ( $r = 0.566$ ,  $P = 0.0001$ ). The novel parameter of vitreous:RPE textural ratio showed a marginally stronger correlation ( $r = 0.604$ ,  $P < 0.001$ ) with clinical vitreous haze scores than the Vitreous:RPE signal ratio.

**Conclusions:** The custom OCT image analysis software (VITAN) allows rapid and automated measurement of vitreous parameters, that is comparable to our previously reported vitreous:RPE index, and correlates with clinically measured disease activity. Such OCT-based indices may provide the much needed objective markers of vitreous activity, which may be used in both clinical assessment, and as outcome measures in clinical trials for intermediate, posterior, and panuveitis.

**Translational Relevance:** We describe a rapid automated method for quantifying vitreous signal intensity on optical coherence tomography (OCT) and show that this correlates with clinical assessment of vitreous inflammation. Such OCT-based indices may provide the much needed objective markers of vitreous activity, which may be used both in routine clinical assessment, and as outcome measures in clinical trials for intermediate, posterior, and panuveitis.

## Introduction

Uveitis, a group of diseases characterized by intraocular inflammation, is a significant cause of blindness worldwide.<sup>1-4</sup> One of the greatest challenges in managing this disorder is the lack of sensitive and objective markers of disease activity.<sup>5,6</sup> This is both an issue in day-to-day clinical management but also hampers all clinical trials in the field. Critically, the major disease activity endpoint for trials in posterior segment-involving uveitis that is recognized by the United States Food and Drug Administration (FDA) and European Medicines Agency (EMA) is the National Eye Institute (NEI) system for grading of vitreous haze.<sup>7,8</sup> Unfortunately, this is limited by being (1) subjective, (2) noncontinuous, (3) poorly discriminatory at lower levels of inflammation, and (4) poorly sensitive in a clinical trial context.<sup>5,6,9</sup>

We recently reported the results of an exploratory study where optical coherence tomography (OCT) imaging was used to provide objective measurement of vitreous inflammation.<sup>10</sup> In this study, a method for quantitative analysis of vitreous signal intensity on OCT was described, and was correlated with clinical vitreous haze scores in patients with uveitis and in healthy volunteers. This method produces a continuous measure of vitreous inflammation, and thus has considerable potential for adoption as a biomarker of uveitic disease activity. Despite this, a significant limitation of our study was the need for manual segmentation of OCT image sets by human graders. While such grading is relatively straightforward, and highly reproducible,<sup>11,12</sup> the requirement for human input nonetheless introduces a subjective element to the process. Perhaps more importantly, manual grading typically requires 5 to 10 minutes for completion, a considerable barrier to any future adoption in clinical practice. Our preliminary study also assessed OCT vitreous signal intensity as a whole, such an intensity assessment would not necessarily encompass the variety of different vitritis patterns seen on the OCTs, which often, for example, have areas of clumping and other varieties of hyperintense inflammatory pixel textures.

To address these concerns, we undertook to develop a software algorithm that can provide both automated analysis of vitreous signal intensity on OCT and other potentially useful OCT measures of vitreous inflammation. In this report, we present a new, dedicated software application for vitreous analysis and assess its use for assessment of patients with uveitis. The application has been designed purely

for the purpose of assessment of vitreous activity from spectral-domain (SD) OCT and is fully automated with no subjective steps. It incorporates a new texture measure designed to improve measurement validity and reliability. Finally, it automatically assesses broader aspects of vitreous inflammation, not measurable by simple intensity, such as vitreous clumping.

## Materials and Methods

### Study Population

Detailed information about the study population and data collected has previously been reported.<sup>10</sup> In brief, data was collected retrospectively from subjects at Moorfields Eye Hospital and the Birmingham & Midland Eye Centre in three categories: (1) eyes with vitreous haze secondary to intermediate, posterior, or panuveitis, (2) eyes with uveitis but with no evidence of vitreous haze, and (3) eyes without evidence of intraocular inflammation or vitreoretinal disease. Approval for data collection and analysis was obtained from a UK National Health Service (NHS) research ethics committee and adhered to the tenets set forth in the Declaration of Helsinki.

### Data Collection

Information about age, sex, diagnosis, and anatomic type of uveitis, were gathered before clinical ophthalmic examination and OCT image acquisition. Best-corrected visual acuity (VA) was measured using Early Treatment Diabetic Retinopathy Study (ETDRS) charts. Clinical ophthalmic parameters assessed included: (1) visually significant keratic precipitates (KPs), (2) posterior synechiae, (3) cataract, and (4) posterior capsular opacification (in pseudophakic eyes). In each eye, the anterior chamber (AC) was graded for cellular activity and flare according to standardized protocols by experienced observers. The presence and severity of vitreous haze was also classified by the same graders according to the NEI system in which clinical examination of the posterior pole is compared against a standard set of photographs.<sup>7</sup> For each eye, OCT image sets were obtained using a SD-OCT system (Spectralis OCT, Heidelberg Engineering, Germany). In each case, volume scans centered on the fovea were obtained.

### Automated OCT Image Analysis

Previous experience informed the development of the new dedicated software application presented in this article, termed “VITAN” (VITreous ANalysis).

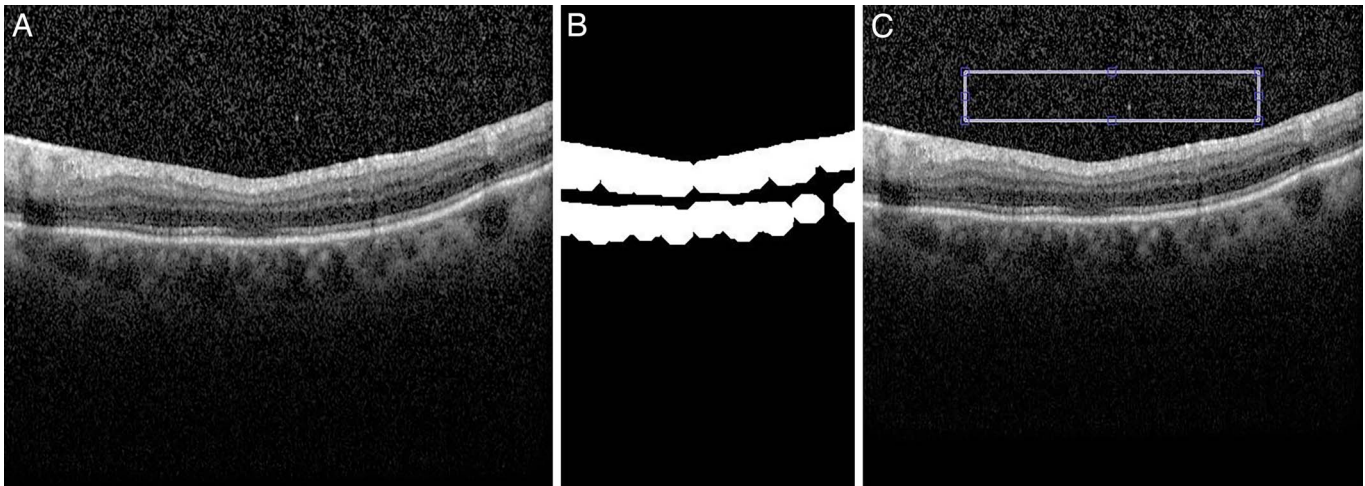


**Figure 1.** (A) Example original image. (B) Binary image of OCT scan automatically segmented to highlight retinal/RPE layers and cropped to isolate central areas. (C) Final automated area of capture overlaid onto original image for user approval.

VITAN is based upon the MATLAB image-processing platform (MathWorks, Natick, MA, USA), and has been designed, developed, and coded to work with Heidelberg Spectralis OCT images.

Once the specific OCT scan required for analysis is loaded into the software, several automated algorithms are initiated. The first stage of the automated processing steps is the application of an image processing morphological technique known as “opening.” This is performed with a small disc-shaped “structuring element” and is followed by subtraction of the resulting area from the original image. The image then has a threshold applied to segment it into a binary form. This algorithm sequence allows for reliable segmentation of the retinal and pigment epithelial layers. It also allows the computer software to precisely define a constructed rectangular area comprising only vitreous tissue just anterior to the macula, for analysis. This constructed area is outlined for the user, who is asked to confirm that it is indeed appropriate vitreous and that the analysis should proceed without interference. Upon confirmation, the analysis is completed without intervention. The software also allows for manual localization of the constructed area if necessary.

Image processing and analysis of this vitreous area then involves three steps, each of which are fully automated. Firstly, as in our previous research paper, the system assesses the mean intensity of pixels in the vitreous relative to that of the previously segmented retinal and pigment epithelial layers. This is performed in order to compensate for overall variations in image gain (e.g., in cases where there is generalized reduction in signal strength from media opacities such as

cataract). Measures other than mean intensity might actually be more robust and valid indicators for inflammation. We, therefore, also developed algorithms using mathematical descriptors of texture relative to retinal pigment intensity, as an alternative approach. Lastly, the system applies algorithms to automatically quantify any tendencies toward clumping of vitreous cells in inflammation; the assessment rectangle area is scanned for high intensity pixels that are adjoining each other. These groups of pixels are labelled by the computer software and subsequently assessed for their number, mean and maximum size. This process is repeated with a higher gain of sensitivity (after a morphological dilation algorithm was applied), to provide two potential scores for vitreous clumping.

All results are automatically transferred to a Microsoft Excel spreadsheet (Microsoft Corp., Seattle, WA). The process is fully automated and the completion of all testing takes less than 2 seconds. The process pauses only to allow the user to verify correct segmentation for the purposes of this investigation but no subjective procedures are required. The computer outputs the mean pixel intensity score after adjustment for retinal pigment epithelium (RPE) levels, and texture analysis indicators of smoothness, also modified according to RPE intensity. Finally, data on vitreous clumping is output.

To produce a final score for each image, three OCT images were analyzed from each eye (the OCT B-scan passing through the foveal center, and the immediately adjacent B-scans), and mean values calculated. An example of the sequence of analysis is given in [Figure 1](#) and in [Table 1](#).



**Table 1.** Objective Outcome Measures From Analysis of Image in Figure 1.

Maths adjusted mean	19.9
Maths adjusted texture	6.68
Number of instances of regions of pixel of greater than 1 pixel	1
Mean area of each region identified above	7
Maximum area of any region identified as above	7
Total number of regions detected of any size	1
Number of instances of regions of pixel greater than 2 pixel	4
Mean area of each region identified by above rules	1.1
Maximum area of any region identified by above rules	3
Total number of regions detected of any size	458

### Reproducibility of Vitreous Analysis

Results were generated by a single researcher (KA). For all images, the software interacted with the user only to request confirmation to proceed with the displayed segmented areas for analysis. For all images analyzed, we recorded whether the displayed areas were deemed correct and whether any such subjective input was required for area correction. A second researcher also assessed whether additional user input was required for any image (TA). For all image processing and analysis, we recorded the number of patients for whom segmentation was deemed correct, thereby avoiding any subjective human intervention.

### Data Analysis and Statistical Methods

Two image processing outcome measures were assessed for each eye: (1) the mean intensity adjusted (MIA) for RPE, and (2) the texture intensity with adjustment (TIA) for RPE. The difference in these values across clinical groupings was first assessed using Kruskal-Wallis one-way analysis of variance by ranks (ANOVA) for nonparametric data. Spearman's rank correlation was then used to assess the relationship between each of these values and the clinical grading of vitreous haze. Other outputs from the analyses were not statistically analyzed in this paper, including vitreous clumping scores, for which numbers of patients were low.

*P* values less than 0.05 were considered statistically significant. Statistical analysis was performed using commercially available software (SPSS, Version 18.0; SPSS Inc., Chicago, IL).

## Results

### Baseline Characteristics

In total, 60 patients (60 eyes) were analyzed. In the main study group (patients with uveitis and evidence of vitreous haze), 30 patients (30 eyes) were analyzed. In the control group, 30 patients (30 eyes) were also evaluated, consisting of 12 patient (12 eyes) with uveitis but without vitreous haze, and 18 patients (18 eyes) without any evidence of uveitis or vitreoretinal disease. A detailed description of the clinical characteristics of the study cohort has been presented previously.<sup>10</sup> Within the main study group of patients with uveitis and evidence of vitreous haze, four eyes were graded as +0.5, 13 eyes as +1, 10 eyes as +2, and three eyes as +3 vitreous haze score.

### Accuracy of Automated Vitreous Segmentation

The software analysis system was easy to use and rapid, with no malfunctions.

Out of 180 total images (three per patient) the user confirmed correct segmentation for all. A second experimenter independently confirmed this finding. For any individual image analysis, therefore, the algorithms are completely automatic with no opportunity for bias or human error and completely identical results would be repeatedly obtained.

### Adjusted Vitreous Mean Intensity and Texture Intensity Values

The TIA values for each clinical category of patient are demonstrated in Figure 2. The distributions were similar enough to proceed to Kruskal Wallis testing. This showed a significant difference for both adjusted means and texture analysis between eyes with uveitis, uveitis with no haze and healthy eyes ( $P < 0.001$ ,  $\chi^2$  statistic 22.6). Spearman's rank correlations between VITAN scores and clinical grading of vitreous haze are presented in Table 2. There was a significant correlation between MIA values and clinical vitreous haze score (coefficient 0.585,  $P < 0.001$ ). A marginally stronger correlation was found between texture analysis of the vitreous and clinical vitreous haze scores (coefficient 0.604,  $P$

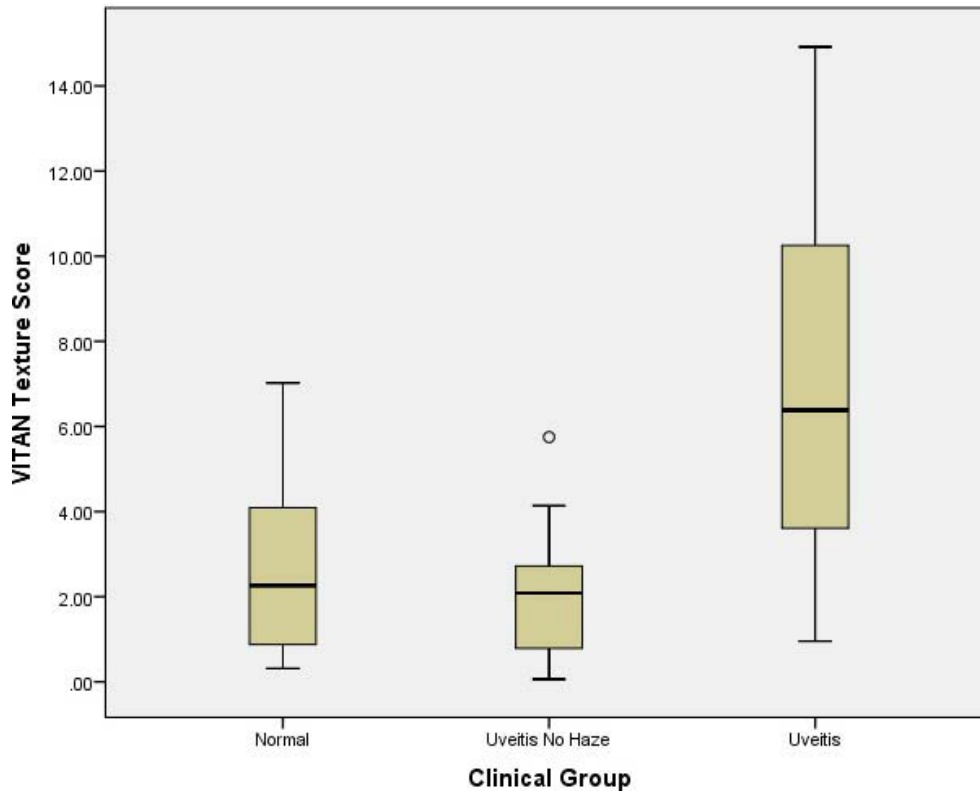


Figure 2. VITAN Texture Scores (TIA) according to clinical category of patient.

< 0.001). Finally, Figure 3 demonstrates a detailed breakdown of MIA and TIA scores for each clinical grade of uveitis.

## Discussion

In this report, we describe the development and application of custom OCT image analysis software, termed VITAN, that allows automated measurement of vitreous parameters in patients with vitreous pathology, and its potential application in the assessment of uveitis involving the posterior segment.

Patients with these forms of uveitis (intermediate, posterior, and panuveitis) typically develop permeation of the vitreous with a protein-rich exudate, which may be assessed by the NEI Vitreous Haze score.<sup>7</sup> Our previous study demonstrated the potential for OCT measurement of vitreous to replace the subjective NEI Vitreous Haze score.<sup>7</sup> In this study we demonstrate that this process can be improved further by moving from manual segmentation and quantification of images to a rapid automated quantification process.

Automated measurements of mean vitreous signal

Table 2. Correlations

			Clinical Score	VITAN Mean Score	VITAN Texture Score
Spearman's rho	Clinical score	Correlation coefficient		.585*	.604*
		sig. (two-tailed)		.000	.000
	VITAN texture score	Correlation coefficient	.604*	.935*	
		sig. (two-tailed)	.000	.000	
	VITAN mean score	Correlation coefficient	.585*		.935*
		sig. (two-tailed)	.000		.000

\* Correlation is significant at the 0.01 level (two-tailed).

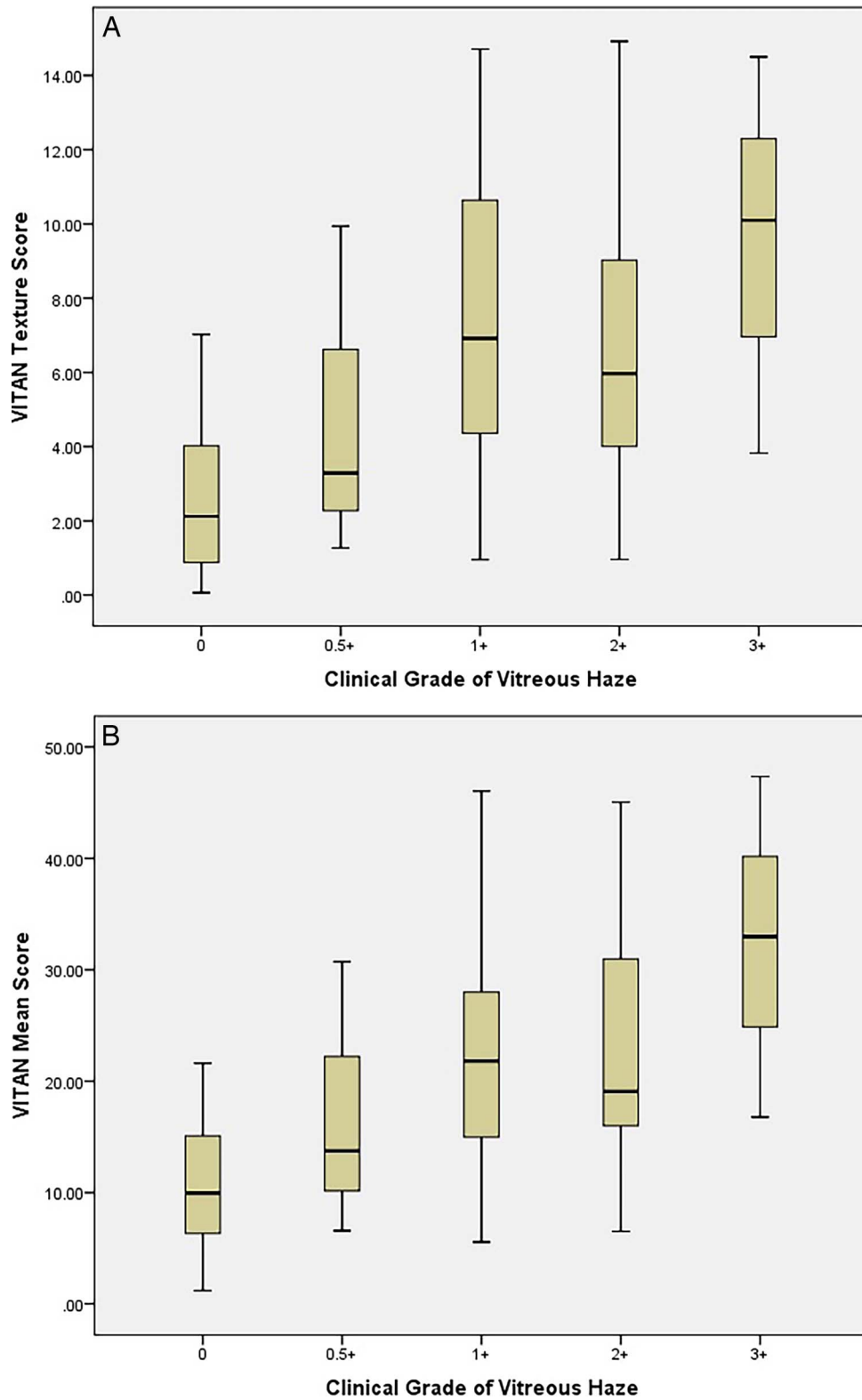
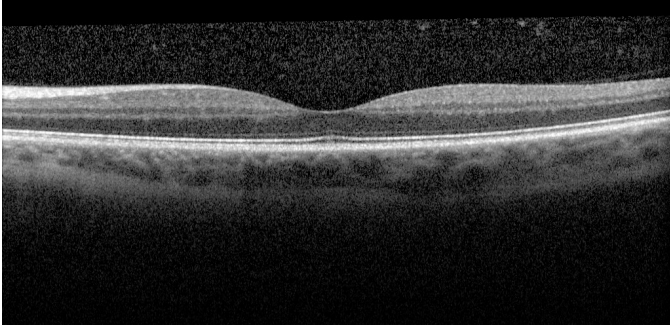


Figure 3. TIA (A) and MIA (B) scores for the detailed different clinical grades of uveitis.



**Figure 4.** OCT demonstrating extensive vitreous inflammation and clumping. The corresponding VITAN scores are high (TIA: 7.1 and MIA: 21.6). Despite this, the clinical vitreous haze score in this example was 0.

intensity, adjusted for mean RPE signal intensity, showed a moderate but significant correlation with clinical vitreous haze scores ( $r = 0.585$ ,  $P < 0.001$ ). This result was comparable to that reported using manual segmentation in our previous study ( $r = 0.566$ ,  $P = 0.0001$ ).<sup>10</sup> We also analyzed the novel parameter of mean vitreous textural intensity, again adjusted for RPE textural intensity (image texture refers to the spatial variation in its pixel intensities and allows quantification of intuitive features such as the “roughness” or “bumpiness” of the image). Using this approach, a marginally superior correlation was found with clinical vitreous haze scores ( $r = 0.604$ ,  $P < 0.001$ ). Finally, we assessed the parameter of vitreous “clumping,” although the number of eyes that demonstrated this feature was too low to perform a detailed statistical analysis. Taken together, these results show considerable promise, particularly given that they are obtained in a fraction of the time required for manual grading (<2 seconds vs. 5–10 minutes) and with greatly increased reproducibility.

As with our original study, the correlations detected with clinical vitreous haze scores are moderate. It should be recognized that clinical vitreous haze scores are not themselves perfect measures of vitreous inflammation and, therefore, any discordance between clinical and OCT analysis of the vitreous may reflect the limitations of either.<sup>13,14</sup> Our method of vitreous textural analysis represents our first attempt at further optimization of our quantitative OCT-derived technique. The dataset utilized in this study was obtained under normal macular scanning conditions. It may be possible to further optimize vitreous OCT scan acquisition using two approaches: (1) “extramacular scanning,” to maximize the volume of vitreous captured, OCT volume scans may be obtained

systematically from peripheral locations,<sup>15</sup> and (2) “enhanced depth vitreous scanning,” to maximize the depth of vitreous captured, the OCT operator can pull back on the joystick during image acquisition. Advances in OCT technology enabling greater volume of vitreous sampling as standard may also facilitate this process. For example, the next generation of “swept-source” OCT technology will allow for greatly increased scanning ranges, with the introduction of vertical cavity surface-emitting lasers (VCSEL) offering the potential to allow greater visualization of the vitreous.<sup>16–18</sup> It will be interesting to compare the results of these optimization techniques/new technologies with the both conventional vitreous haze scores, and newer approaches, such as the nine-point, graded, photograph-to-photograph technique utilized in the MUST trial.<sup>13,14,19</sup> Given the well-documented limitations of clinical vitreous haze scores,<sup>5,6,9,19</sup> it may also be useful to perform more detailed analyses of specific cases where there is a disparity with vitreous OCT parameters. For example, in the example patient shown in [Figure 4](#), increased vitreous reflectivity and clumping of vitreous aggregates is seen. Accordingly, the VITAN scores were high (TIA 7.1, MIA 21.6). Despite this, the NEI clinical vitreous haze score in this example was 0.

Our results suggest that some patients without clinical evidence of uveitis can have moderately elevated vitreous intensity measures on OCT. This may be related to age-related condensations of the vitreous,<sup>20</sup> or to intrinsic limitations of our software, or of OCT imaging itself. It is also conceivable that vitreous OCT intensities could be elevated in a variety of retinal diseases, for example, increased vitreous concentrations of vascular endothelial growth factor (VEGF) may result in increased level of proteinaceous exudation within the vitreous. This hypothesis is being explored by our group in a separate study. Therefore, the software application described in this report is, as of yet, intended as a tool for measuring disease activity and response to treatment rather than as a diagnostic tool per se. As such, we have not attempted to calculate diagnostic sensitivities or specificities. It must also be borne in mind that the complications of uveitis (e.g., vitreous hemorrhage in the context of retinal vasculitis) or coexistent pathology may also increase the reflectivity of the vitreous space, and that this must be considered when interpreting such scans.

It is hard to over-emphasize the need for better outcome measures in uveitis for use in both routine clinical practice and in the evaluation of emerging



therapies.<sup>5,6,9</sup> OCT provides an exciting opportunity to quantify vitreous changes in an objective manner, using noninvasive technology that is already used as standard in ophthalmic clinics. Automated quantification such as VITAN demonstrates that this can be achieved in routine practice and not just as a research tool. Ideally, for such a marker to be considered for adoption by trialists and regulatory authorities as a surrogate endpoint in clinical trials of this disease, it would first be shown to correlate with disease outcome in patients with uveitis.<sup>21–23</sup> This is likely to be challenging, and indeed validation studies for both the NEI Vitreous Haze score and the nine-point, graded, photograph-to-photograph technique focused on issues of inter- and intraobserver reliability rather than visual function. Indeed in their validation study using the nine-point photographic study to analyze baseline data in the MUST trial, Madow et al.<sup>14</sup> note that “It is unknown whether changes in the vitreous haze score over time will correlate with outcomes of known significance such as vision, so that haze can be considered a legitimate outcome measure for clinical trials.” Due to the multiple ways in which uveitis (and sometimes its treatment) impacts the ocular tissues and consequently impairs visual function,<sup>6</sup> compounded by the irreversible nature of some of these changes, it is not surprising that both trials and clinical experience demonstrate that there is imperfect correlation between markers of disease activity (such as vitreous haze) and measures of visual function (such as visual acuity).<sup>9,14</sup>

The applications of automated quantification of vitreous intensity may also extend beyond noninfectious uveitis to other forms of ocular pathology in which vitreous changes are relevant either as an outcome measure or where more detailed characterization may inform us of the natural history of the disease, ranging from the severe (such as endophthalmitis) to the more benign (e.g., asteroid hyalosis, vitreous syneresis, etc.). Within uveitis, future studies will assess the implications of vitreous clumping analyses and study varying locations of texture and mean intensity vitreous analysis considering whether assessments centrally may vary compared with assessments nearer the uveal tract. A key clinical application will be to study progression in uveitis, and other vitreous-involving pathologies, to aid determination of clinical change. Studies are underway to assess this. Although many further exploratory and clinical assessments are needed, it is hoped that the continued development of this application will lead to important clinical benefits in aiding those involved in

the complex task of assessing and managing patients with intraocular inflammation and uveitis.

## Acknowledgments

This research was funded by National Institute of Health Research and facilitated by the Manchester Biomedical Research Centre, the Greater Manchester Comprehensive Local Research Network and a Fight For Sight UK/Olivia’s Vision Uveitis Small Grant Award (principal investigator: Dr. Denniston). Drs. Keane and Sim have received a proportion of their funding from the Department of Health’s NIHR Biomedical Research Centre for Ophthalmology at Moorfields Eye Hospital and UCL Institute of Ophthalmology. The views expressed in the publication are those of the author and not necessarily those of the Department of Health.

\* Extended OCT-Quantification of Uveitis Activity for Trial Outcomes and Reporting (EQUATOR). For full list of contributing authors and affiliations of authors from the EQUATOR Consortium please see [Appendix](#).

Disclosure: **P.A. Keane**, member of the Allergan European Retina panel, educational presentations for Novartis, Bayer, Allergan, Topcon, Heidelberg; **K. Balaskas**, received educational and travel grants from Bayer and Novartis; **D.A. Sim**, member of the Allergan European Retina panel, received travel grants from Allergan; **K. Aman**, none; **A.K. Denniston**, none; **T. Aslam**, received educational and travel grants from Novartis, Bayer, Thea, Bausch & Lomb, and research grants from Bayer and Thea

## References

1. Durrani OM, Meads CA, Murray PI. Uveitis: a potentially blinding disease. *Ophthalmologica*. 2004;218:223–236.
2. Wakefield D, Chang JH. Epidemiology of uveitis. *Int Ophthalmol Clin*. 2005;45:1–13.
3. Nussenblatt RB. The natural history of uveitis. *Int Ophthalmol* 1990;14:303–308.
4. Rothova A, Suttorp-van Schulten MS, Frits Treffers W, Kijlstra A. Causes and frequency of blindness in patients with intraocular inflammatory disease. *Br J Ophthalmol*. 1996;80:332–336.



5. Lin P, Suhler EB, Rosenbaum JT. The future of uveitis treatment. *Ophthalmology*. 2014;121:365–376.
6. Denniston AK, Dick AD. Systemic therapies for inflammatory eye disease: past, present and future. *BMC Ophthalmol*. 2013;13:18.
7. Nussenblatt RB, Palestine AG, Chan CC, Roberge F. Standardization of vitreal inflammatory activity in intermediate and posterior uveitis. *Ophthalmology*. 1985;92:467–471.
8. Jabs DA, Nussenblatt RB, Rosenbaum JT. Standardization of Uveitis Nomenclature Working Group. Standardization of uveitis nomenclature for reporting clinical data. Results of the First International Workshop. *Am J Ophthalmol*. 2005;140:509–516.
9. Kempen JH, Ganesh SK, Sangwan VS, Rathinam SR. Interobserver agreement in grading activity and site of inflammation in eyes of patients with uveitis. *Am J Ophthalmol* 2008;146:813–818, e1.
10. Keane PA, Karampelas M, Sim DA, et al. Objective measurement of vitreous inflammation using optical coherence tomography. *Ophthalmology*. 2014;121:1706–1714.
11. Joeres S, Tsong JW, Updike PG, et al. Reproducibility of quantitative optical coherence tomography subanalysis in neovascular age-related macular degeneration. *Invest Ophthalmol Vis Sci*. 2007;48:4300–43097.
12. Sadda SR, Joeres S, Wu Z, et al. Error correction and quantitative subanalysis of optical coherence tomography data using computer-assisted grading. *Invest Ophthalmol Vis Sci*. 2007;48:839–848.
13. Davis JL, Madow B, Cornett J, et al. Scale for photographic grading of vitreous haze in uveitis. *Am J Ophthalmol*. 2010;150:637–641, e1.
14. Madow B, Galor A, Feuer WJ, et al. Validation of a photographic vitreous haze grading technique for clinical trials in uveitis. *Am J Ophthalmol*. 2011;152:170–176, e1.
15. Keane PA, Allie M, Turner SJ, et al. Characterization of birdshot chorioretinopathy using extramacular enhanced depth optical coherence tomography. *JAMA Ophthalmol*. 2013;131:341–350.
16. Keane PA, Sadda SR. Retinal imaging in the twenty-first century: state of the art and future directions. *Ophthalmology*. 2014;121:2489–2500.
17. Grulkowski I, Liu JJ, Potsaid B, et al. High-precision, high-accuracy ultralong-range swept-source optical coherence tomography using vertical cavity surface emitting laser light source. *Opt Lett*. 2013;38:673–675.
18. Grulkowski I, Liu JJ, Zhang JY, et al. Reproducibility of a long-range swept-source optical coherence tomography ocular biometry system and comparison with clinical biometers. *Ophthalmology*. 2013;120:2184–2190.
19. Hornbeak DM, Payal A, Pistilli M, et al. Interobserver agreement in clinical grading of vitreous haze using alternative grading scales. *Ophthalmology*. 2014;121:1643–1648.
20. Itakura H, Kishi S. Aging changes of vitreomacular interface. *Retina*. 2011;31:1400–1404.
21. Csaky KG, Richman EA, Ferris FL III. Report from the NEI/FDA ophthalmic clinical trial design and endpoints symposium. *Invest Ophthalmol Vis Sci*. 2008;49:479–489.
22. Lloyd R, Harris J, Wadhwa S, Chambers W. Food and Drug Administration approval process for ophthalmic drugs in the US. *Curr Opin Ophthalmol*. 2008;19:190–194.
23. Taylor RS, Elston J. The use of surrogate outcomes in model-based cost-effectiveness analyses: a survey of UK Health Technology Assessment reports. *Health Technol Assess* 2009;13:iii, ix-xi, 1-50.

## Appendix

EQUATOR Consortium members who contributed to this study comprise:

Tariq Aslam<sup>1,2,3</sup>, Alastair K. Denniston<sup>4,5,6</sup>, Andrew D. Dick<sup>7,8</sup>, Michael Karampelas<sup>7,9</sup>, Pearse A. Keane<sup>7</sup>, Richard W. Lee<sup>7,8</sup>, Philip I. Murray<sup>5,6</sup>, Robert B. Nussenblatt<sup>10</sup>, Carlos E. Pavesio<sup>7</sup>, Srinivas R. Sadda<sup>11</sup>, H. Nida Sen<sup>10</sup>, Dawn A. Sim<sup>7</sup>, Adnan Tufail<sup>7</sup>

<sup>1</sup>Manchester Royal Eye Hospital, Central Manchester University Hospitals NHS Foundation Trust, Manchester Academic Health Science Centre, Manchester, UK

<sup>2</sup>Faculty of Medical and Human Sciences, University of Manchester, UK

<sup>3</sup>School of Built Environment, Herriot-Watt University, UK

<sup>4</sup>Queen Elizabeth Hospital Birmingham, University Hospitals Birmingham NHS Foundation Trust, Birmingham, UK

<sup>5</sup>Academic Unit of Ophthalmology, University of Birmingham, Birmingham, UK

<sup>6</sup>Birmingham & Midland Eye Centre, Sandwell and West Birmingham NHS Trust, Birmingham, UK

<sup>7</sup>NIHR Biomedical Research Centre for Ophthalmology, Moorfields Eye Hospital NHS Foundation Trust and UCL Institute of Ophthalmology, UK

<sup>8</sup>Academic Unit of Ophthalmology, University of Bristol, Bristol, UK

<sup>9</sup>Hinchingbrooke Hospital, Hinchingbrooke Health Care NHS Trust, UK

<sup>10</sup>National Eye Institute, National Institutes of Health, Bethesda, Maryland, USA

<sup>11</sup>Doheny Eye Institute, University of California, Los Angeles (UCLA), USA